REMARKS

In the final Office Action, the Examiner rejected claim 31 as anticipated by the Shinohe et al. reference, rejected claims 16, 20 – 23, 25 – 20 (sic, should be 16, 20 – 23, 25 - 30) and 32 as obvious over the Shinohe et al and Hshieh et al. references, and rejected claim 24 as obvious over Shinohe et al. and Hshieh et al. in view of Hsu et al.

35 U.S.C. §102(e)

The **Shinohe et al.** reference shows one floating guard ring in Figure 12, for example. Little is said in the reference about the function of the floating guard ring. The floating guard ring of the type shown in Shinohe is of a conventional construction and is known in the art. Such floating guard rings are also known as floating field rings.

To better illustrate the function of such floating guard rings, Applicants enclose a reference work for the Examiner's review. In particular, a copy of pages 92 – 100 of the teaching text book, "Modern Power Devices," by B.J. Baliga, 1987, John Wiley and Sons, is enclosed as Appendix 1 for the Examiner's consideration.

In section 3.6.2 beginning on page 92, the Baliga work explains the function of floating field rings, or floating guard rings. The floating guard rings of the type show in the cited Shinohe reference and as described in the Baliga reference are used to shift the boundary of the space charge region to the edge. The floating guard rings do not result in the charge carriers being depleted. By extending the space charge region to the outer edge, the effective curvature of the blocking pn-junction of the active region is decreased. By decreasing the

effective curvature, the break down voltage of the pn-juntion of the active region is increased. This is the so-called "surface-effect".

By contrast, the present invention is directed to an edge termination which is based on the volume effect. The volume effect, although not referred to as such, is explained in further detail in U.S. Patent No. 5,216,275, a copy of which is enclosed for the Examiner's review as Appendix 2. As is apparent after review of the aforementioned patent, the effect of depleting a layer consisting of n-regions and p-regions where the n-regions and p-regions contribute to charges with opposite signs is discussed in detail. The doping concentrations of these n-regions and p-regions are designed in such a way as that the blocking condition of the whole layer is totally depleted.

The concept as discussed in the U.S. Patent No. 5,216,275 is used in the present invention in an edge termination region.

The claims of the present application define the invention in such a way that it is distinguished over the cited art of Shinohe. As such, the claim 31 is not anticipated thereby.

35 U.S.C. §103(a)

Even when the teachings of Shinohe is combined with the Hshieh et al. reference alone or when the combination is considered in view of Hsu et al., the claimed invention is still not found or suggested. In particular, adding the teaching of parallel connected components of Hshieh does not make up the differences between the Shinohe reference and the present invention. Contrary to the Examiner's statements on page 4, bottom, and page 6, bottom, to page 7, top, of the final action, the conductivities and geometries of Shinhohe are not set so

that their free charge carriers are totally depleted when a blocking voltage is applied, even when considered in combination with Hshieh.

The addition of the electrode material of Hsu does not result in the combined teachings of the Shinohe reference and the Hshieh reference disclosing or even suggesting the present invention.

The present invention as claimed is thus not shown or suggested in the prior art, and therefore is a non-obvious improvement thereover.

Conclusion

Each issue raised in the final action has been addressed. Early favorable reconsideration and allowance is hereby requested.

Respectfully submitted,

Melvin A. Robinson (Reg. No. 31,870)
Schiff Hardin & Waite
Patent Department
6600 Sears Tower
Chicago, Illinois 60606
Telephone: 312-258-5785
CUSTOMER NO. 26574
ATTORNEY FOR APPLICANT

CERTIFICATE OF MAILING

I hereby certify that this correspondence is being deposited with the United States Postal Service as First Class Mail in an envelope addressed to:

Commissioner for Patents
P.O. Box 1450
Alexandria, VA 22313-1450

on October 7, 2003.

CH1\4056695.1

This Page Is Inserted by IFW Operations
and is not a part of the Official Record

BEST AVAILABLE IMAGES

Defective images within this document are accurate representations of the original documents submitted by the applicant.

Defects in the images may include (but are not limited to):

- BLACK BORDERS
- TEXT CUT OFF AT TOP, BOTTOM OR SIDES
- FADED TEXT
- ILLEGIBLE TEXT
- SKEWED/SLANTED IMAGES
- COLORED PHOTOS
- BLACK OR VERY BLACK AND WHITE DARK PHOTOS
- GRAY SCALE DOCUMENTS

IMAGES ARE BEST AVAILABLE COPY.

As rescanning documents *will not* correct images,
Please do not report the images to the
Image Problem Mailbox.

MODERN POWER DEVICES

B. JAYANT BALIGA

General Electric Company
Schenectady, New York

APPENDIX 1

A Wiley-Interscience Publication
JOHN WILEY & SONS

Copyright © 1987 by John Wiley & Sons, Inc.

All rights reserved. Published simultaneously in Canada.

Reproduction or translation of any part of this work beyond that permitted by Section 107 or 108 of the 1976 United States Copyright Act without the permission of the copyright owner is unlawful. Requests for permission or further information should be addressed to the Permissions Department, John Wiley & Sons, Inc.

Library of Congress Cataloging in Publication Data:

Baliga, B. Jayant, 1948-
Modern power devices.

"A Wiley-Interscience publication."
Includes bibliographies and index.
1. Power electronics. 2. Power semiconductors.
3. Power transistors. 4. Semiconductor rectifiers.
I. Title.
TK7881.15.B35 1987 621.38 86-15891

Printed in Singapore

10 9 8 7 6 5 4 3 2

To

My wife

the background doping level. The breakdown voltage of spherical junctions can be derived from the critical electric field at breakdown. Normalization of this voltage to the parallel-plane case gives a general expression that is independent of the background doping level:

$$\frac{BV_{SP}}{BV_{PP}} = \left(\frac{r_j}{W_c}\right)^2 + 2.14\left(\frac{r_j}{W_c}\right)^{6/7} - \left[\left(\frac{r_j}{W_c}\right)^3 + 3\left(\frac{r_j}{W_c}\right)^{13/7}\right]^{2/3} \quad (3.57)$$

This expression is plotted in Fig. 3.16 for comparison with the cylindrical junction. In general, the breakdown voltage of the spherical junction is found to be about a factor of 2 times lower than that of the cylindrical junction. The creation of spherical junctions at device terminations must, therefore, be avoided. Since the spherical junction is caused by the presence of sharp corners, as at the edges of the rectangular diffusion window in Fig. 3.11, such junctions can be avoided by rounding the devices edges. However, this results in loss in the active junction area by

$$\text{Area loss} = (4 - \pi)R^2 \quad (3.58)$$

where R is the radius of curvature of the corner. To obtain the full benefits of rounding the corners during mask design, it is essential to make the radius of curvature R several times larger than the depletion width at breakdown.

3.6.2. Floating Field Rings

It is apparent from the previous section that the fabrication of devices using planar technology could lead to a serious degradation in the breakdown voltage as a result of high electric fields at the edges. An elegant approach to reducing the electric field at the edges is by using floating field rings [9]. The term floating field rings was coined because they consist of diffused regions that are isolated

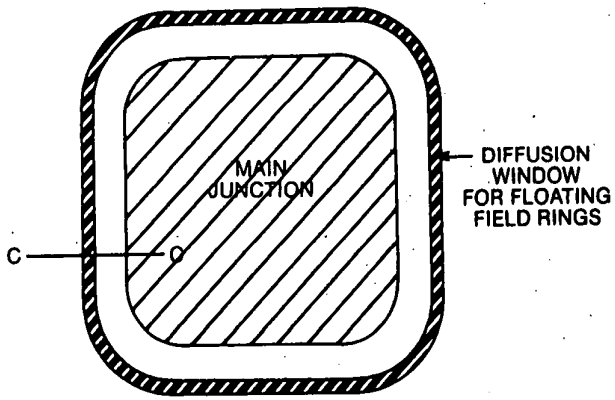

from the main junction but located close to it. These regions can assume a potential intermediate to that of either side of the P–N junction. Their potential is established by the depletion layer extending from the main junction. These floating field rings are almost invariably fabricated simultaneously with the main junction because this can be achieved in the same processing step during device fabrication by creating an extra diffusion window in the mask that surrounds the main junction as illustrated in Fig. 3.20. It is important to retain a uniform spacing between the main junction and the floating field ring.

When the floating field ring is fabricated simultaneously with the main junction, their diffusion depths will be equal. A cross section of this structure taken along line C–C is illustrated in Fig. 3.21*a*. A cross section of a junction without the floating field ring is shown in Fig. 3.21*b* for comparison. It can be seen that the electric field crowding responsible for the low breakdown voltage of cylindrical junctions is reduced by the presence of the floating field ring. During reverse-bias operation of the main junction at low voltages, its depletion layer is small and does not extend to the floating field ring. The floating field ring then retains the potential of the lightly doped P region. As the reverse bias on the main junction increases, its depletion layer widens until it punches through

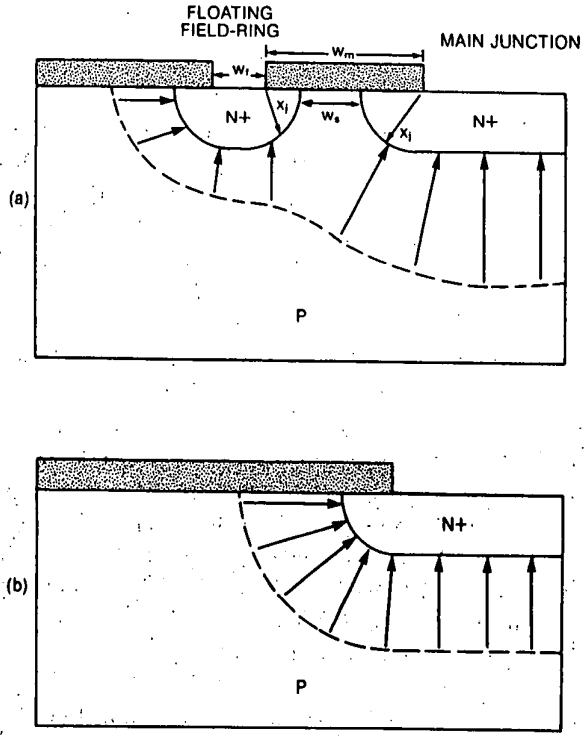

Fig. 3.21. Comparison of the electric field crowding for a planar junction (*a*) with and (*b*) without

to the floating field ring. The voltage at which this occurs is related to the minimum spacing W_s between the floating field ring and the main junction. If the lateral diffusion of the junction is assumed to be equal to the vertical depth, the mask dimension W_m used for the location of the floating field ring relative to the main junction can be calculated from the punch-through voltage V_{PT} by using the relationship

$$W_m = 2x_j + W_s = 2x_j + \sqrt{\frac{2\epsilon_s V_{PT}}{qN_A}} \tag{3.59}$$

Once the punch-through occurs, the potential on the floating field ring tracks the main junction potential. As an extreme case, if a floating field ring is considered that is infinitesimally small in width [27], it will not have any effect on the voltage distribution in the depletion layer. Its potential can then be related to the main junction potential by using Eq. (3.14):

$$V_{ffr} = \frac{qN_A}{\epsilon_s}\left(W_d W_s - \frac{W_s^2}{2}\right) \tag{3.60}$$

where W_d is the depletion width of the main junction, which is related to the main junction voltage V_a by Eq. (3.15), and the subscript ffr denotes floating field ring. Combination of Eqs. (3.15) and (3.60) yields

$$V_{ffr} = \sqrt{\frac{2qN_A}{\epsilon_s} W_s^2 V_a} + \frac{qN_A}{2\epsilon_s} W_s^2 \tag{3.61}$$

The floating field ring potential varies as the square root of the applied potential on the main junction for this case. In the case of actual floating field rings that distort the electric field distribution, it has been found that the floating field ring potential varies as the 0.65th power of the reverse bias on the main junction.

Although the floating field ring can be intuitively expected to increase the breakdown voltage by reducing the electric field crowding, its exact location relative to the main junction is crucial to its effectiveness in increasing the breakdown voltage. If the floating field ring is placed too far away from the main junction, it will have little effect on the depletion layer curvature at the main junction. Breakdown will then occur at the main junction without a substantial increase from the cylindrical case. If the floating field ring is placed too close to the main junction, its potential will be nearly equal to that of the main junction. Breakdown will then occur at the field ring at nearly the same voltage as without the field ring. However, optimal placement of the floating field ring can result in nearly a twofold increase in the breakdown voltage [10].

The breakdown voltage of planar junctions with optimally placed floating field rings has been analyzed numerically. An example of the effect of the floating field ring location on the breakdown voltage is shown in Fig. 3.22. Here the breakdown voltage has been normalized to the parallel-plane case and the field ring spacing has been normalized to the depletion layer width on the lightly doped side of the junction. It can be seen that the optimal floating field ring

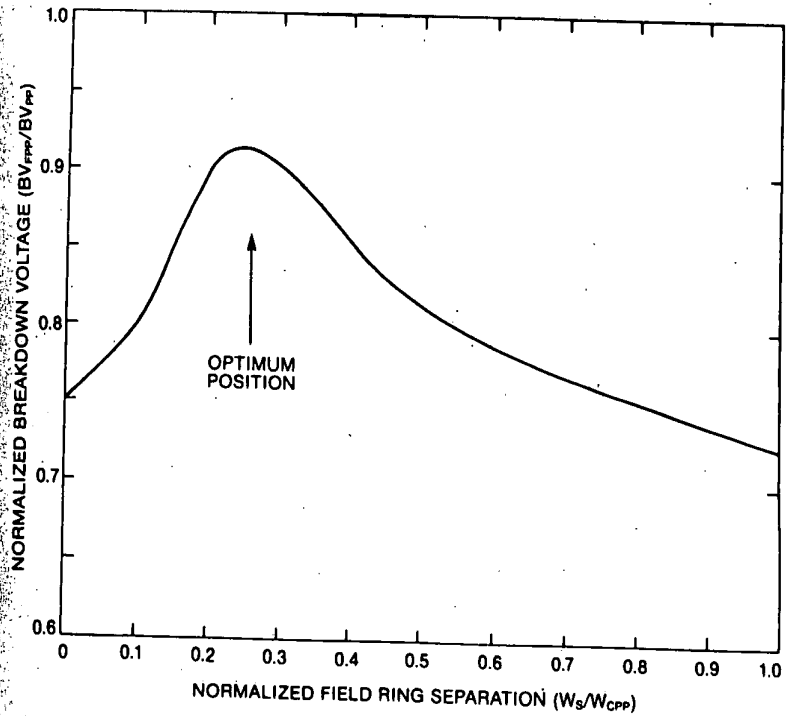

Fig. 3.22. Effect of floating field ring position relative to the main junction on its breakdown voltage.

location for this case is about 0.25 times the depletion layer width at breakdown on the lightly doped side for the parallel-plane case. An important point to note in Fig. 3.22 is that the breakdown voltage predicted by the numerical analysis shows a sharply pointed distribution around the optimal spacing. This implies that, to obtain the full benefits of a single floating field ring, it is essential to precisely control the mask dimension W_m and the junction depth of the diffusion. In general, this can be easily achieved during device design and fabrication.

The optimal spacing indicated in Fig. 3.22 is based on the assumption that there is no charge at the surface of the semiconductor over the lightly doped region. The presence of surface charge has a strong influence on the depletion layer spreading at the surface because this charge complements the charge due to the ionized acceptors inside the depletion layer. Examples of the depletion layer shape for the case of positive, zero, and negative surface charge are provided in Fig. 3.23 for a planar junction. Positive surface charge causes the depletion layer at the surface of the lightly doped side to extend further, whereas negative charge will tend to retard the depletion layer. The opposite effect will apply to a junction with a lightly doped N-type region. For the cylindrical junction illustrated in Fig. 3.23, the presence of positive surface charge will

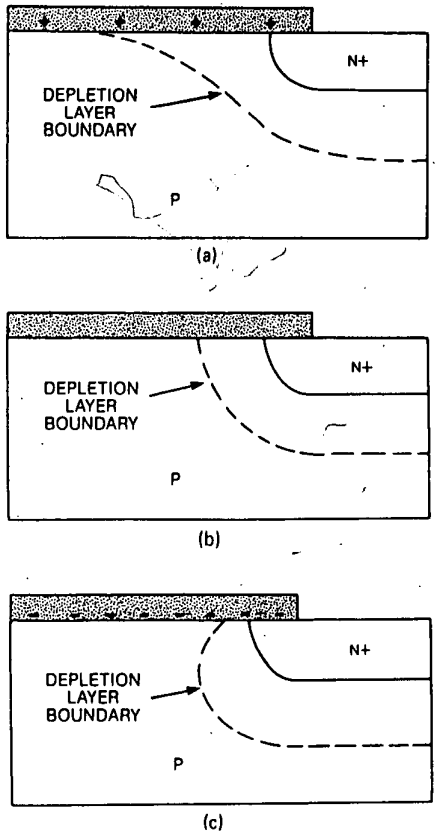

Fig. 3.23. Influence of surface charge on depletion layer spreading at the edge of a planar junction: (*a*) positive charge; (*b*) zero charge; (*c*) negative charge.

breakdown voltage, whereas negative surface charge will have the opposite effect. Thus positive charge is beneficial for the simple planar junction with a lightly doped *P* region. In the case of junctions with field rings, however, surface charge of either polarity can lower the breakdown voltage because it affects the punch-through voltage to the floating field ring. This alters the optimal spacing and results in lowering the breakdown voltage because of the sharply peaked breakdown voltage distribution around the optimum spacing. If the surface charge is precisely known, it is possible to analyze for the optimal floating field ring location, including the effect of this charge, and then design the mask spacing W_m. In practice, the charge at the surface of thermally oxidized silicon is positive and in the range of 10^{10} to $10^{12}/cm^2$. Even with a well-controlled, clean fabrication sequence for a complex device such as a power MOSFET, the surface charge will vary from wafer to wafer and even across a wafer by $\pm 1 \times 10^{11}/cm^2$. This represents an inherent practical limitation to designing the

Under the assumption that the floating field ring is optimally located with respect to the main junction, the breakdown voltage has been found to be enhanced by nearly a factor of 2 over the simple cylindrical planar diffused junction. Through use of the same normalization scheme adopted in the earlier sections for cylindrical and spherical junctions, it has been found that the breakdown voltage of all junctions with floating field rings can be represented by a single line as shown in Fig. 3.24. The breakdown voltage of cylindrical junctions without the floating field ring is included in this figure for comparison. The impact of the floating field ring is the greatest for high voltage devices fabricated by use of shallow junctions. For these junctions with small $r_j/W_{c,PP}$, where the breakdown voltage is less than 30% of the parallel-plane case, the addition of

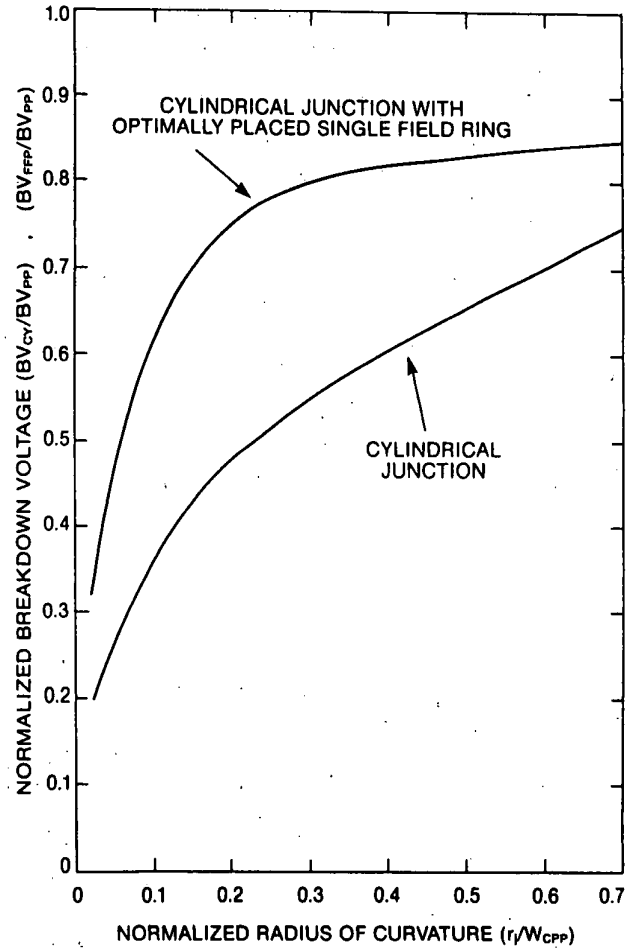

Fig. 3.24. Normalized breakdown voltage of planar junctions with single optimally placed floating

the floating field ring can raise the breakdown voltage by a factor of nearly 2. For deep junctions, where the curvature effects are small to begin with, the addition of the floating field ring will raise the breakdown voltage by a much smaller amount. Since the floating field ring can take up valuable space on the periphery of the device and reduce the utilization of chip area, its use is more commonplace in small devices operating at low voltages (<1500 V).

The optimal spacing of floating field rings was discussed in the preceding section. Another design parameter that is important is the width W_f of the window through which the floating field region is diffused into the semiconductor. If the width of the window W_f is very small, the floating field ring can become ineffective in reducing the depletion layer curvature even when it is at the optimal location. This is illustrated in Fig. 3.25*a*. To be fully effective in raising the breakdown voltage, it is necessary to make the width of the floating field ring comparable to the depletion layer width. Making the floating field ring width much larger than the depletion layer width, as shown in Fig. 3.25*b*, is not advisable because it does not improve the breakdown voltage but results in wasting space at the edge of chip.

The floating field ring concept, with its extensions using multiple rings or field plates, represents the most widespread device termination technique for the small field controlled devices discussed in this book. Its design is crucial

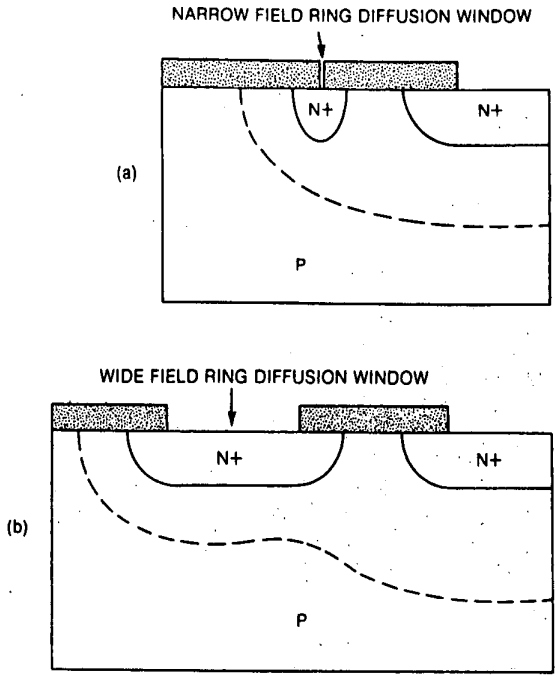

to achieving the high-performance ratings that have been reported for power MOSFETs.

3.6.3. Multiple Floating Field Rings

Since a single field ring reduces depletion layer curvature and the electric field crowding, it can be expected that several floating field rings working in conjunction with each other may raise the breakdown voltage even closer to the parallel-plane case. As in the case of the single floating field ring, multiple floating field rings are generally fabricated with the main junction by designing the mask with multiple windows surrounding the main junction.

Two design philosophies exist for designing the multiple floating field ring termination. In one case the spacing between individual floating field rings is varied together with its width. The floating field ring spacing and its width should both decrease with increasing distance from the main junction. This provides a gradual extension of the depletion layer away from the main junction as illustrated in Fig. 3.26. The field rings further away from the junction can be made narrower because the depletion layer depth below them becomes progressively smaller, thus saving space at the device periphery. However, this approach is based on the assumption that the surface space charge is precisely known, and the field ring spacings are designed by including the effect of this space charge. If the surface space charge in the actual device is more positive than that assumed during device design, the inner field rings can become ineffective, transferring all the voltage to the outer field rings and resulting in premature breakdown at the outer field ring. In the ideal case, these field rings will all share the applied voltage equally, producing avalanche breakdown at the outer edges of all the floating field rings simultaneously.

In the second design approach, all the floating field rings are made narrow and are equally spaced. Because of the smaller width of these floating field rings and their closer spacing, more of them can be accommodated within a given

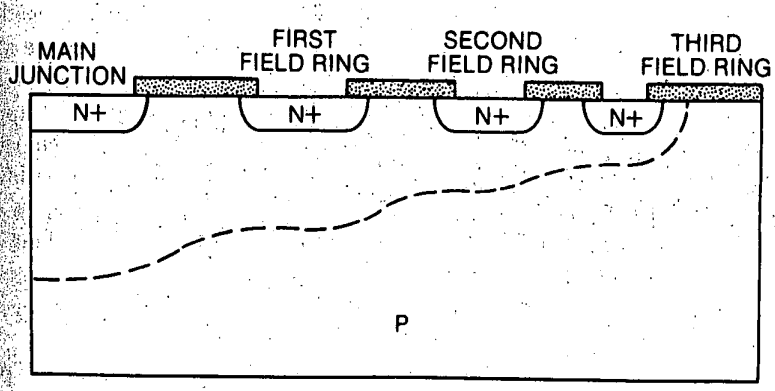

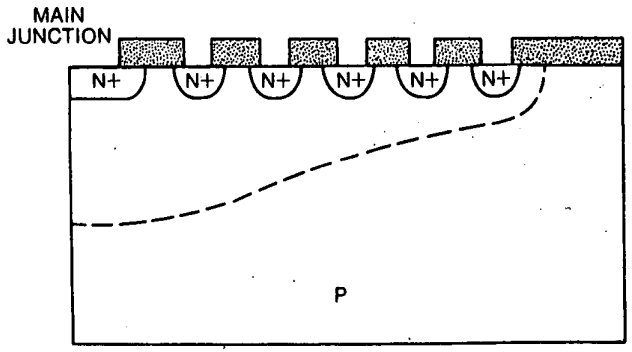

Fig. 3.27. Multiple field ring termination with equal width and spacing.

edge area as shown in Fig. 3.27. This design produces a much finer gradation in the depletion layer at the edge of the device. The design of this termination is also easier because it is essentially based on use of the minimum design rules when laying out the windows and spacings that control the field ring spacing and width. This termination is also sensitive to the surface charge, but the presence of a larger number of rings reduces the impact of surface charge variations when compared to the earlier multiple field ring design.

Through application of these multiple floating field ring designs, the breakdown voltage can be raised arbitrarily close to the parallel-plane case. The only limitation to applying this approach lies in the space taken up at the edge of the chip. In practical devices, it is usual to use three floating field rings. Designs with up to 10 floating field rings have been utilized where it is important to achieve close to the parallel-plane junction breakdown.

3.6.4. Beveled-Edge Terminations

With the application of solid-state thyristors to power control, there has been a constant need to develop higher-voltage devices. It was apparent during the early stages of thyristor development that it was necessary to design edge terminations that promote bulk breakdown. Since these high-voltage, large-area devices were manufactured by using gallium and aluminum diffusions to obtain highly graded deep junctions, planar termination techniques were not applicable. It was instead necessary to bring the junction to the edges of the chip and provide adequate surface passivation to avoid premature surface breakdown.

The simplest approach was to make the device edge perpendicular to the wafer surface. This can be done by either sawing or scribing and breaking the wafer. This approach creates considerable surface damage at the edges of the chip which is difficult to passivate. Furthermore, it was discovered that cutting the edge of the wafer at an angle improved the breakdown voltage.

Consider the case of a junction whose area at the edge decreases when pro-

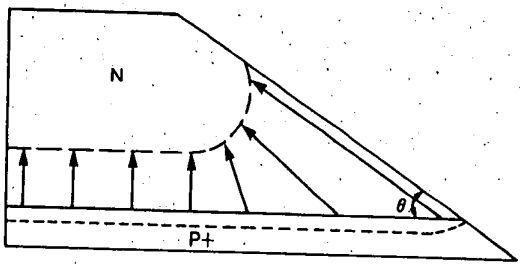

Fig. 3.28. Positive-bevel-edge contour.

is known as a *positively beveled junction* and is illustrated in Fig. 3.28. The depletion layer shape and corresponding electric field distribution are also indicated in this figure. To maintain the charge balance on the opposite sides of the junction, the depletion layer on the lightly doped side of the junction is forced to expand near the surface. This expansion of the depletion layer causes a reduction in the electric field crowding. Since the depletion layer width along the surface is much larger than in the bulk, it can be concluded that the electric field along the surface will be much smaller than that in the bulk. This is an ideal design for the termination of junctions because it ensures bulk breakdown prior to surface breakdown if the surface electric field is sufficiently low. It should be noted that even if the surface electric field is lower than in the bulk, surface breakdown may precede bulk breakdown because the ionization coefficients at the surface are generally larger than in the bulk for the same electric field strength because of the presence of defects at the surface.
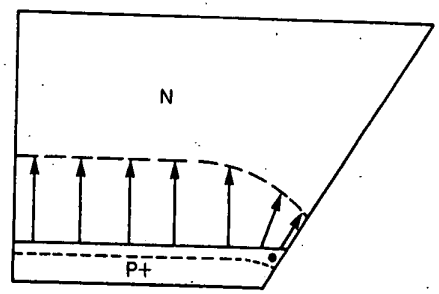
If the edge of the junction is cut in the opposite direction so that the area of the junction increases when proceeding from the highly doped side toward the lightly doped side, the contour is known as a *negative-beveled junction.* The depletion layer shape for this case is illustrated in Fig. 3.29. The establishment of charge balance on the opposite sides of the junction causes the depletion layer at the surface of the lightly doped side to decrease while the depletion layer on the heavily doped side expands. If the diffused side of the junction is heavily doped, the depletion layer shrinkage on the lightly doped side will have